Process-induced strains measurements through a multi-axial characterization during the entire curing cycle of an interlayer toughened Carbon/Epoxy prepreg

Rima Sfar Zbed, Steven Le Corre, Vincent Sobotka

Process-induced strains measurements through a multi-axial characterization during the entire curing cycle of an interlayer toughened Carbon/Epoxy prepreg

Rima Sfar Zbed[a], Steven Le Corre[a,*], Vincent Sobotka[a]

[a] *Université de Nantes, CNRS, Laboratoire de thermique et énergie de Nantes, LTeN, UMR 6607, F-44000 Nantes, France.*

Abstract

High dimensional accuracy of thermoset composite parts is a challenging issue for manufacturers in the aeronautical industry. A deep understanding of the cure behavior is required in order to prevent internal stresses generation as being responsible of shape deformations. However, the specific challenge of experimental investigations is to cover all of the stages of the cure process including the pre-gelation region. In this paper, the characterization of the process-induced strains throughout the cure is based on using a laboratory scale bench named as PvT-HADDOC. Tests were performed on a unidirectional interlayer toughened aerospace prepreg. The device enables the measurements of the induced strains simultaneously along the out-of-plane and the in-plane directions. The consolidation of the uncured material is captured. The measured coefficients of thermal expansion are proved to be higher through the thickness direction in the liquid and cured states. The chemical shrinkage is measured before and after gelation along both transverse directions. The orthotropic behavior of IMA/M21 system is attributed to the presence of interleaf layers of resin within the prepreg plies.

Keywords: A. Prepreg, B. Anisotropy, B. Thermomechanical, E. Cure

*Corresponding author at: Université de Nantes, CNRS, Laboratoire de thermique et énergie de Nantes, LTeN, UMR 6607, F-44000 Nantes, France.

Email addresses: rima.sfar-zbed@univ-nantes.fr (Rima Sfar Zbed), steven.le-corre@univ-nantes.fr (Steven Le Corre), vincent.sobotka@univ-nantes.fr (Vincent Sobotka)

1. Introduction

Because of their various advantages, thermosetting composites have been the composite of choice for several years in diverse sectors. They have been applied increasingly in the aerospace industry with a particular important usage of carbon-epoxy prepregs that represent the baseline material for aircraft primary structures such as the case of the AIRBUS A350 [1]. Aerospace-grade composites made of toughened epoxy prepregs have been in some way of certain concern. They are commonly termed as third generation since they incorporate thermoplastic particles either into the epoxy matrix as a dissolved phase or as undissolved particles distributed on the prepreg surface to form toughened resin rich areas as interleaves [2]. This technique of interleaving has been widely used as a solution to enhance cured laminate composites toughness. It is assumed to give significant improvements of the inter-laminar toughness and the mechanical properties such as the static strength and fatigue resistance [3]. During processing, the thermosetting matrix undergoes several transitions. The resin transforms from a viscous fluid to a rubbery viscoelastic solid and eventually a glassy solid. This transition from an uncured liquid to a solid state is called gelation upon which the material modulus starts to build up. During this stage, a three-dimensional network of cross-linked chains of molecules is formed associated to an increase of the resin viscosity and a decrease in the free space occupied by the polymer molecules which is usually referred to as chemical shrinkage.

Autoclave manufacturing is the most common fabrication process of composite structures based on high performance aerospace-grade prepregs. During this process, prepreg layers are cured under prescribed cycles with controlled temperature, pressure and vacuum. Quality of parts is mainly influenced by manufacturing as the material undergoes various multi-physical phenomena throughout all the process stages including prepreg layup, vacuum bagging and curing. Hence, it is important to select the appropriate cycle for each particular application to reduce the process induced defects and enhance dimensional accuracy

of components. Trial-and-error methods have been largely required to compensate the mold geometry for the expected distortions. However, it involves a big amount of testing and generates very costly manufacturing trials. For this reason, models are developed to simulate the fabricating process and predict the cure behavior of thermosetting composite layups. Residual stresses are among the major reasons that trigger shape distortions of parts especially when generated at the macro scale as detailed in the review proposed by Baran et al. [4]. Among the described phenomena that are proved responsible of the internal stress creation we can cite thermal anisotropy of individual plies and thus of the lay-up, chemical shrinkage and consolidation considered as intrinsic properties of the material in addition to the tool–part interaction effect as an extrinsic parameter that takes place due to the mismatch of the Coefficient of Thermal Expansion (denoted as CTE hereafter) between the mold and the composite part during curing. Hence, information about the CTE to account for the thermal effect and the Coefficient of Chemical shrinkage (denoted as CCS hereafter) to characterize the cure behavior are of big importance when modeling the processing of composites. Fine measurements of these parameters are required since the validity of most models must be determined by experimental tests to assess the accuracy of the predicted phenomena. CTE and CCS are difficult properties to measure on a reacting composite sample. Indeed, several of the different tested techniques presented in the literature were conducted on pre-cured or fully cured materials to overcome some experimental limitations. There have been a number of experimental methods carried out to investigate these phenomena and most of them have been discussed in [5–8], the most popular will be briefly outlined below.

Chemical shrinkage of thermosetting resin and associated composites have been widely characterized in a common way by investigating the volumetric behavior through volume dilatometric methods. Among the most used techniques, (PVT)-type dilatometers were employed to provide global information about the chemical behavior of isotropic thermosetting resins and also of fiber reinforced thermoset composites [9–11]. Many studies involved the use of the PvT-α mold

that allowed the characterization of the global volume chemical shrinkage and the estimation of the volumetric CTE of thermoset resins and thermosetting composites [12, 13]. Even though this device proved to be useful, there remains a need for an efficient method that can enable directional measurements of the linear properties related to the thermo-chemical behavior of thermoset composites. Dynamic Mechanical Analysis (DMA) [14] was employed by some authors in order to measure dimensional changes during cure. Despite its satisfying results, this method is only limited to partially or fully cured prepreg samples that are tested under conditions which are by no means representative of the manufacturing process. Several studies reported the use of optical fiber sensors placed directly inside the composite parts such as Fiber Brag Grating (FBG) [15, 16] and Distributed Optical Sensors (DOS) [17] to monitor cure shrinkage and thermal expansion. Unfortunately, the information about local strains estimated by these methods are only limited to the post-gelation stage of the curing behavior.

Thermal mechanical analyzer (TMA) has been used by several authors for measurement of chemical shrinkage in thermoset composites [18, 19]. Garstka et al. [19] used a similar system of a TMA to investigate the through-thickness dimensional variations of unidirectional and cross-ply samples made of a toughened epoxy prepregs. It was possible to estimate the post-gelation cure shrinkage. Additionally, during the pre-gelation regime, a drop in strains was noticed and the induced compaction was attributed to the consolidation of the material. In a different study, an other way to investigate the thermo-chemical strains was introduced by Duffner et al. [20] [6] using Digital Image Correlation (DIC). The reported results showed the ability of the method to estimate not only the transverse in-plane CTE and CCS but also the compaction behavior of the sample that occurs at the pre-gelation stage. It was observed that a notable strain drop took place during the heating step. The authors suggested that the observed compaction is related to the self-consolidation of the material since there is no pressure applied during the curing tests. The latter was assumed to be only induced by the effects of surface tension and the resulting capillary

pressure that could drive the resin saturation associated to the viscosity drop with increasing temperature that allows flow. In spite of the limitations of the two last methods to be performed under atmospheric pressure and their ability to capture the evolution of the thermo-chemical strains through only one direction, the observed findings about consolidation highlighted the requirement for greater understanding of this phenomenon that occurs at the pre-gelation regime. Indeed, consolidation of composite laminates has also a significant impact on the final shape of parts. Much research were conducted to understand and model the development of this phenomena to prevent stress-strain generation during cure and part distortions. As stated in [21, 22], it is assumed to be dominated by the resin flow considered as responsible for removing excess resin and eliminating voids. The compaction of the fiber bed and the resin flow are assumed to take place simultaneously in autoclave process and the two phenomena thoroughly influence each other [22, 23]. Experimental investigations on uncured prepregs are still required to understand the compaction behavior during consolidation of these materials.

The purpose of this study is therefore to present a new experimental procedure that aims to characterize a unidirectional interlayer toughened Carbon/Epoxy prepreg during the entire cure cycle in order to better understand the complex behavior during processing, including the early pre-gelation stage. To achieve this objective, the approach adopted here is based on the investigation of the induced strains throughout the consolidation of the uncured material and the induced thermo-chemical strains. In a first step, the reaction kinetic of the same neat epoxy resin is modeled in order to be able to estimate the degree of cure and to obtain a better understanding of the shrinkage development of the studied material during curing. The induced strains during the cure of the studied prepreg are measured in a second step through a multi-axial characterization carried out using a laboratory scale bench. The estimation of the CTE is based on the analysis of the thermal induced strains measured in the uncured and cured states. The dependency of the chemical shrinkage on the cure temperature is studied and the CCS of the material are finally estimated.

2. Materials and cure kinetics

2.1. The Carbon/Epoxy prepreg

This study was conducted with a unidirectional aerospace-grade prepreg supplied by Hexcel Composite, HexPly®M21/34%/UD194/IMA−12K. This prepreg is made of M21 epoxy resin and IMA carbon fibers with a nominal cured ply thickness of 0.184 mm [24]. The IMA/M21 system is a toughened prepreg that includes extra layers of resin incorporating undissolved thermoplastic particles as distinct interleaves between plies as illustrated in Fig. 1.

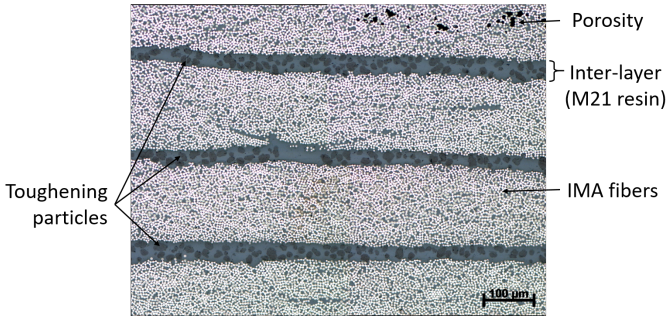

Figure 1: Micrograph of the thickness of the IMA/M21 laminate cured sample.

2.2. The M21 Epoxy resin

2.2.1. Cure kinetics

The HexPly®M21 epoxy resin used in the impregnation of the supplied prepregs was also provided by Hexcel. This so-called neat resin includes in fact the thermoplastic particles present in the interleaf layers of the IMA/M21 laminates. It has been largely characterized in the literature and the cure kinetics was modeled by different authors. Phenomenological models are generally preferred to study the M21 epoxy system as they empirically describe reactions in comparison to the mechanistic models which are much more complex [7, 25]. Relying on the investigation conducted by Abou Msallem et al. [26] to model the cure reaction of the same type of resin, the proposed autocatalytic model of Bailleul et al. [27] was used in this research to predict the evolution of the

degree of cure of our material for any imposed thermal history. It describes the polymerization rate through a combination of Arrhenius and polynomial functions. It has been extended by Abou Msallem et al. [26] to consider the effects of the glass transition temperature on the polymerization rate as detailed in the following equations

$$\begin{cases} \frac{d\alpha}{dt} &= G(\alpha) \cdot K_A(T) \cdot K_D(T,\alpha) \\ G(\alpha) &= \sum_{i=0}^{i=7} a_i \cdot \alpha^i \\ K_A(T) &= K_{ref} \cdot exp\left(-A\left(\frac{T_{ref}}{T} - 1\right)\right) \\ K_D(T,\alpha) &= K_2 \cdot exp\left(C_1\left(\frac{T - T_{g(\alpha)}}{C_2|T - T_g(\alpha)|}\right)\right) \\ T_g(\alpha) &= T_{g0} + \frac{(T_{g\infty} - T_{g0}) \cdot \lambda \cdot \alpha}{(1-(1-\lambda)\cdot\alpha)} \end{cases} \quad (1)$$

where α is the degree of cure, dα/dt is the crosslinking rate and G(α) is a polynomial function. K_A(T) is the Arrhenius law that describes the dependence of the cure rate on temperature (T) and K_D(T, α) is an exponential function that describes the effect of glass transition on the diffusion of macromolecules and the cure kinetics rate [28] where $T_{g\infty}$ and T_{g0} are the glass transition temperature for the cured and uncured resins respectively and λ is a material constant. The values of the constants are given in Table 1.

Table 1: Parameters of the kinetics model [26].

G(α)	a_0 = 0.88	a_1 = 1.81	a_2 = -5.48	a_3 = 29.26
	a_4 = 138.39	a_5 = -232.08	a_6= 177.59	a_7= -52.37
K_A(T)	T_{ref} = 493.13 K	K_{ref} = 0.00164 s^{-1}	A = 19.113	
K_D(T)	K_2 = 0.335	C_1 = 2.3	C_2 = 60 K	
$T_g(\alpha)$	$T_{g\infty}$ = 215° C	T_{g0}=-4.15° C	λ = 0.551	

Model adequacy was verified on the M21 resin using the PvT-α mold during the curing under a constant pressure of 50 bars and according to the manufacturer's recommended thermal cycle. One should mention that such high pressure applied around the neat resin sample was used as recommended in previous work conducted on PvT-α mold and detailed in [29] and has no particular

effect on the resin thermo-chemical behavior during the cure. Resin samples have an initial thickness of 6 mm and diameter equal to 44 mm. The thermal cycle consists of a heating ramp of 2°C/min up to 180°C followed by an isothermal curing dwell of 120 min. As outlined in the introduction, this specific characterization device (described in previous publications [11, 12, 26]) can simultaneously measure the heat flux, the surface temperature and the volumetric dimension changes of the resin sample. Fig. 2 shows an example of the measured heat flux plotted versus time, together with the prescribed thermal cycle. The experimental degree of cure obtained by integration of the heat flux is compared to the estimated one using the kinetic model (the reproducibility of the results was checked on 2 samples). As indicated in Fig. 2, there is a good agreement between experimental data and the model prediction for the degree of cure which validates the choice of the model for our M21 resin system.

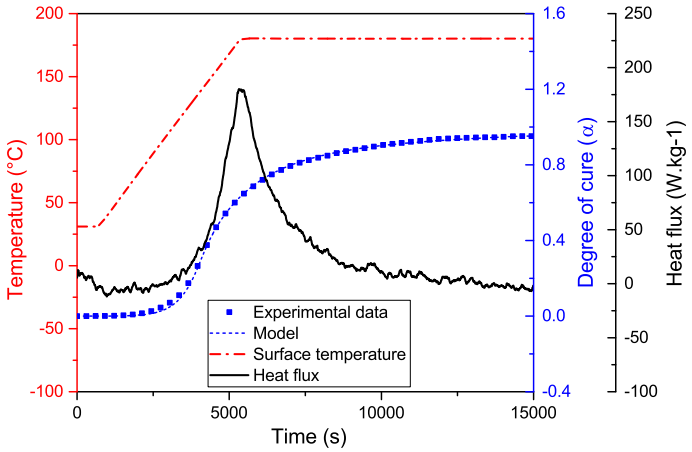

Figure 2: Comparison between the degree of cure estimated with the PvT-α mold measurements and the predicted one by the chosen model (Eq. 1). (For interpretation of the references to color in this figure legend, the reader is referred to the web version of this article.)

3. Experimental set-up and methods

3.1. The PvT-HADDOC device

In this study, the characterization of the process-induced strains throughout the cure of the IMA/M21 prepreg is conducted using an already existing home-made laboratory scale bench named as PvT-HADDOC for Pressure, Volume and Temperature - Homogeneous Anisotropic Deformation and Degree Of Cure monitoring. The PVT-Haddoc experiments presented in this work use homogeneous mechanical and thermal conditions as it will be detailed in the next paragraphs. The aim of this characterization is therefore to provide an analysis of the intrinsic behavior of thermosetting composites during the cure, independently of the particular bagging conditions commonly used in the case of autoclave curing process. A detailed description of the working principle of the first version of this device can be found in a previous work carried out by Péron et al. [30]. An outline of the principal components and the experimental protocol adopted in this work is presented in this section.

Design. This bench consists of a mold cavity assembled to an Instron ElectroPuls E10000 electrical press as illustrated by Fig. 3. The research presented in this paper is based on some important improvements of the first version aimed at enabling a homogeneous thermal and mechanical state around the samples while curing.

Thermal control. During the experiment, the curing of the tested samples takes place inside of the mold cavity which is filled up with a CALSIL IP 50 silicon oil. The sample is placed between the piston which is assembled to the moving frame of the machine and a plate that is attached to the lower heat exchanger of the cavity (see Fig. 3-*right*). The selected thermal cure cycle is ensured by both heat exchangers that are connected to a Vulcatherm thermo-controller unit that allows the heating/ cooling of the system by circulating a heating oil through these exchangers. A PT100 sensor is placed in one of the exchangers and serves as input for the thermo-controller PID. The applied

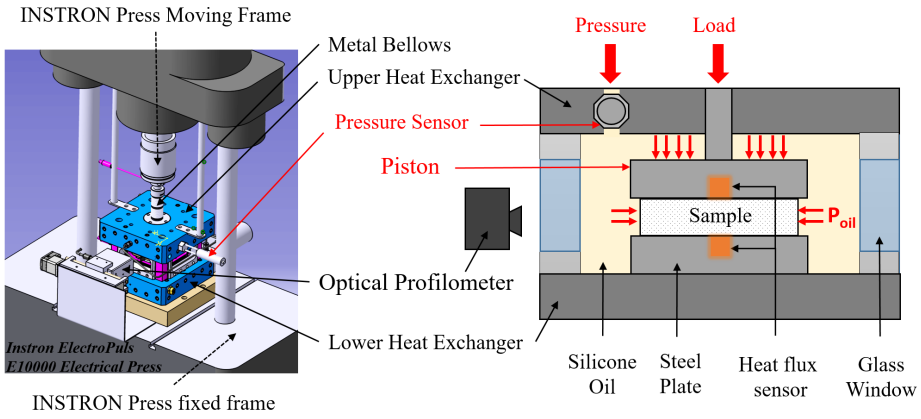

Figure 3: Global overview of the PvT-HADDOC experimental setup. 3D conception (*left*) and a scheme of the mold cavity (*right*).

temperature can reach up to 200°C. The silicon oil circulates continuously inside the mold cavity and through both exchangers thanks to a pump inserted inside the cavity in order to provide the thermal homogeneity around the sample. A PT100 sensor is also placed in the cavity so as to control the oil temperature during curing. As presented in Fig. 3-*right*, two heat flux sensors are embedded in the piston and the steel plate so that they are in contact with the upper and lower sample surfaces, respectively. Data treatment of these sensors, as described in [30], provides information about the surface temperatures of the sample and the heat flux exchanged between the latter and the device. Those sensors enable to calculate the experimental degree of cure of the sample by analyzing these fluxes during the chemical reaction of the material.

Mechanical state. A compressive homogeneous hydrostatic stress is applied around the sample throughout the whole cure cycle assuming that the friction on its surfaces is negligible. As it can be seen from Fig. 3, the sample is simultaneously submitted to the compressive force applied by the piston along its thickness combined to the lateral oil pressure. The latter is controlled by an external piston allowing to reach 10 bars during the cure and monitored by a local high temperature pressure transmitters 35X HTC inserted in the mold cavity.

In order to properly impose the isotropic compressive state, an additional force is applied by the piston in order to compensate exactly the pressure lack due to its diameter. By doing so, the normal stress in the thickness is perfectly adjusted to the value of the oil pressure value inside the cavity.

Displacement measurements. It is possible to record the dimensional variations of an anisotropic thermosetting composite sample during the cure process simultaneously along two directions. **The in-plane** measurements are provided by a laser profilometer KEYENCE LJ-V 7080 placed in front of the glass window of the mold cavity. It enables the recording of the displacements of the sample lateral surface as a function of time with a resolution of 0.5 μm. Refraction phenomena occur while the received rays propagate through the three different transparent media, *i.e.* ambient air, glass window and silicone oil as the emission and the reception zones of the profilometer are not coincident. Thus, the estimation of the transverse in-plane deformations of the sample throughout the cure requires an optical correction of the raw data coming from the profilometer as it was detailed and validated by Péron et al. [30]. In addition, due to the thermal expansion of the mold cavity including the glass window, a second correction of the measured displacements is needed to overcome thermal expansion effects in the in-plane direction. For further details about the correction techniques involved in this study, the reader is refereed to [30]. The laser sensor allows the recording of the lateral surface variation through vertical lines (about 39 mm in length along axis 3) parallel to the thickness of the sample as shown in the representative illustration of the emitted laser beam in Fig. 5. As the profilometer could move along axis 1, it was possible to record the evolution of the in-plane displacements (along axis 2) for several positions throughout the width of the sample. In our case, only three positions along axis 1 were chosen: x_1 = -5 mm, x_2 = 0 mm, x_3 = 5 mm. Thus, throughout a curing cycle, the sensor sweeps along the three positions continuously at 5 mm.s-1 with a sampling frequency of 10 Hz. **The through-thickness** measurements of the sample dimensional variations are given by the displacement of the piston recorded by

the Instron Press Optical Encoder that enables a linear resolution of 1 nm. The piston is monitored in constant force mode during the total cure process which enables to follow the variation of the sample thickness. The estimation of the through-thickness strains relies on a correction of the raw data recorded by the press through a baseline-test performed without any sample and under the same conditions in order to remove the thermal expansion effects related to the device.

3.2. Samples preparation and manufacturing

All the tested samples made of the IMA/M21 prepreg were stacked into a unidirectional configuration by hand lay-up. A representative laminate is shown in Fig. 4 and 1, 2, 3 are the three main directions of a UD prepreg laminate. Hereafter, axis 1 runs parallel to the direction of fibers, axis 2 will be referred to the in-plane transverse direction and axis 3 defines the through-thickness transverse direction. All the samples were made of 30 plies. For each specimen, squares of 140 $\times$ 140 mm^2 were firstly cut from the prepreg, laid-up and then placed on a flat aluminum tool and covered with a vacuum bag. The removal of air forces the bag down onto the stacked laminate ensuring a debulking pressure of up to 1 atmosphere. All the tested samples were debulked at room temperature during 2 hours, then cut again to obtain the final sample shape with in-plane dimensions of 105 $\times$ 105 mm^2. The average initial thickness was 5.95 $\pm$ 0.05 mm. Before inserting the sample in the device, the steel plate and the piston were lubricated with silicone oil grease as it was detailed and validated by Péron et al. [30] in order to ensure a frictionless contact between the surfaces and the sample during the cure.

The manufacturer's recommended thermal cure cycle for our samples thickness consists of a heating ramp of 2°C/min up to 180°C followed by an isothermal curing of 120 min at this temperature before the cooling step at 2°C/min. The applied pressure during curing according to autoclave processing for this aerospace-grade material is commonly 7 bars which corresponds to the saturated vapor pressure of water at 180°C to prevent the development of porosity.

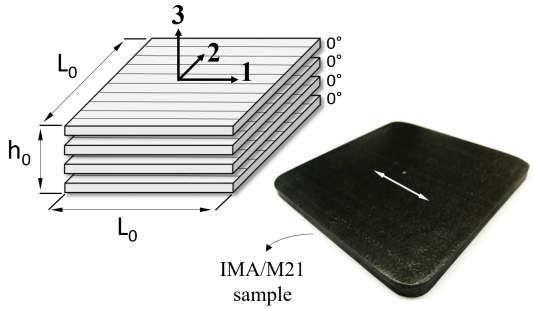

Figure 4: Coordinate system and dimensions for a unidirectional IMA/M21 prepreg sample.

As the objective is to examine the whole curing behavior, a particular interest is given to the pre-gelation stage in this work. In order to get rid from the voids compaction phenomenon that can be observed in the early stages of heating, the standard cycle was modified by adding an isothermal dwell at 70°C during 50 min. By doing so, the compaction being completed, the thermal expansion in the uncured state could be properly observed. The study of this initial consolidation step will not be detailed here, as the focus is set on the intrinsic expansion and shrinkage behavior of this composite.

The effect of the curing temperature on the induced chemical shrinkage was assessed by testing two temperatures 160°C and 180°C. During the heating steps of the material, 2 heating ramps were performed 2°C/min and 4°C/min which were chosen to be in line with the curing temperatures 180°C and 160°C, respectively. Cycle II is aimed at enabling the chemical reaction to start only during the isothermal dwell since a higher heating rate leads the onset of the crosslinking reaction to take place at a higher temperature. Thereby, by separating the cure effects from the thermal expansion, one can also avoid the conflicting effects of both mechanisms during the heating stage. However, one should mention that the polymerization rate at 160°C is much lower than at 180°C. Therefore, the isothermal dwell at 160°C for cycle II is applied during 210 min in order to enable the investigation of the post-gelation chemical shrinkage which will lead to a different maximum degree of cure of about 83% compared to 92% for cycle I. The applied pressure for samples (1) cured at 180°C was 7

bars. On the other hand, samples (2 - 4) were cured at 160°C under 5 bars. This pressure was chosen to correspond approximately to the saturated vapor pressure of water at 160°C in order to prevent voids growth as recommended in [25, 31] and therefore to ensure the same curing conditions for the tested samples. Details regarding the two adjusted curing cycles examined during this study and each of the tested sample are listed in Table 2.

Table 2: Details for the adjusted cure cycles and specimen used in this study.

Cycle Number	Steps	Starting Temperature	Heating Ramp	Hold Temp /Time	Cooling Ramp	Applied Pressure	Tested sample number
I	1/2	30°C (15min)	2°C/min	70°C/50min		7 bars	1
	2/2	70°C	2°C/min	180°C/120min	2°C/min		
II	1/2	30°C (15min)	2°C/min	70°C/50min		5 bars	2, 3, 4
	2/2	70°C	4°C/min	160°C/210min	2°C/min		

4. Results and discussion

4.1. Transverse in-plane displacement measurements

Raw data captured by the optical profilometer were corrected in order to estimate the real induced displacements. Sample 2, cured according to cycle II is taken as an example to illustrate displacements evolution with time along axis 2 reported in Fig. 5 for a given position among the three swept positions by the sensor (here x = 0). The measured displacements of the sample's lateral surface are given by means of a measuring segment (axis 3) along the through-thickness direction of about 4 mm long along axis 3. Through the selected measuring line, we can follow the material induced displacements throughout different points (20 points per mm). In Fig. 6, 5 points with different positions along the measuring line were extracted and the induced in-plane displacements are plotted versus time. The proposed cure cycle consists in a first heating step until t = 2100 s from 30°C to 70°C and a first isothermal hold during 50 min that does not advance the chemical reaction of the material. Displacements are zeroed after this step (at t = 5100 s) in order to account for the new reference

state obtained after voids compaction. A second heating ramp up to 160°C at 4°C/min is applied until t = 6450 s. During this stage, it can be seen that all the displacements follow the same evolution and increase with the temperature due to thermal expansion. During the isothermal cure at 160°C, the drop in the measured displacements indicates the chemical shrinkage phenomenon. From t = 19000 s, the displacements decrease following the cool-down step. As visible from these results, the displacements evolution for the 5 selected points reveal a homogeneous in-plane deformation along the thickness of the sample. It is noted that the same results were found for the three swept positions of the lateral surface by the sensor along axis 1. From this, the in-plane strains during the cure were calculated by averaging the induced displacements along the selected measuring line for the three positions of the sensor.

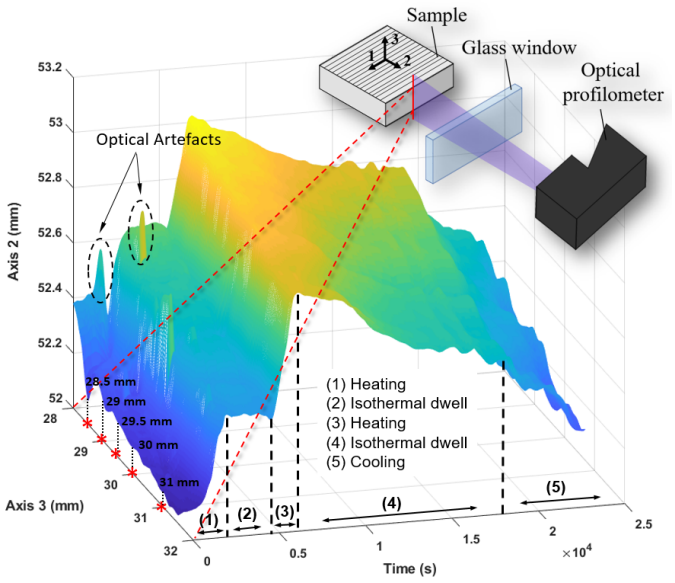

Figure 5: In-plane raw displacements evolution of the lateral surface of *sample - 2* along the measuring line with time for a selected position of the sensor.

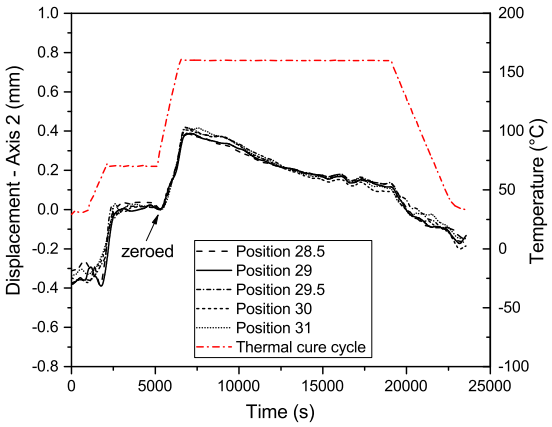

Figure 6: Evolution of the in-plane displacements for the 5 selected points along the through-thickness measuring line with time.

4.2. Evolution of the cure-induced strains along the three directions

Raw displacements were exploited and the deformations along the three directions were calculated as follows

$$\varepsilon_{33}(t) = \frac{\Delta h(t)}{h_0} \quad and \quad \varepsilon_{11,22}(t) = \frac{\Delta L(t)}{L_0/2} \tag{2}$$

where $\Delta h(t)$ is the through-thickness displacement measured at time t after correction of raw data with the baseline test, $\Delta L(t)$ is the in-plane displacement measured at time t after applying the optical correction of raw data and subtracting the overall thermal expansion effects of the device, h_0 is the initial thickness of the sample and L_0 is the initial in-plane dimension.

The entire curing behavior of the studied material is presented in Fig. 7. Samples (2 - 4) cured according to cycle II are taken as examples. The curing induced strains of samples 2 and 3 are presented to demonstrate the good reproducibility of results. The measured strains along both transverse directions are given together with the thermal cycle and the simulated degree of cure. In order to assess the anisotropic dimensional variations along the three directions of space, the in-plane strain through the longitudinal direction of sample 4 was recorded thanks to the optical profilometer. Only the induced in-plane strains of this sample are shown in Fig. 7 for the sake of clarity. The curing behavior

of prepregs is typically divided into two phases, before and after gelation of the matrix. In view of the results presented here, we suggest a further breakdown of the pre-gelation stage. Therefore, the induced strains will rather be analyzed depending on the evolution of the material state in line with the thermal cycle and physical phenomena that drive the cure behavior during the entire cycle. Consequently, 4 stages can be distinguished as indicated in Fig. 7.

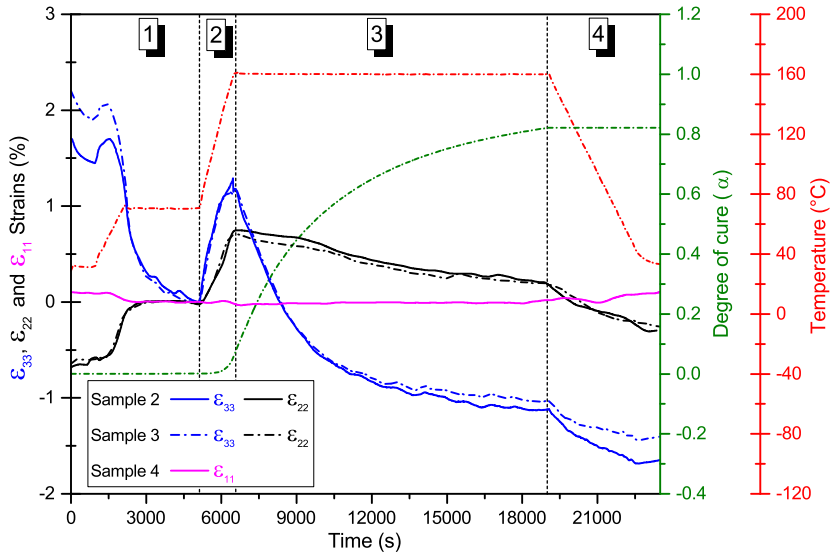

Figure 7: Comparison between the deformations along three directions together with the estimated degree of cure and the thermal cure cycle.

During **'stage 1'** the material was heated up to 70°C and held during 50 min under isotropic compressive pressure of 5 bars. Along the longitudinal direction, the ε_{11} strains show a small contraction which can be attributed to the negative coefficient of thermal expansion of carbon fibers that controls the thermal effects in the axial direction. Typically, during heating, one would expect an expansion through the transverse directions for a unidirectional material. The studied prepreg exhibits a through-thickness contraction illustrated by a significant drop in the ε_{33} strains. Indeed, the thickness decrease starts to take place steadily during the first isothermal dwell of 15 min at 30°C. A slight increase in the ε_{33} strains is then observed due to thermal effects. The shrinkage begins

at the early stage of heating and persists until the end of the isothermal step. Conversely, through the transverse in-plane direction, the material is likely to follow the thermal cycle as visible from the increase in the ε_{22} strains. One can presume that it only compacts through its thickness during this stage. As it is still uncured, the main competing mechanisms in this region are therefore compaction and thermal expansion which develop differently in both transverse directions. Additional experiments, not presented here, were already been conducted with various thermal cycles in order to separate both phenomena in the uncured state as a single heating ramp could not enable the assessment of the thermal expansion of the liquid material. When an isothermal dwell was held for a sufficient time at a high temperature level, the material was observed to reach a limit of compaction and the phenomenon was likely to end. However, an isothermal hold at higher temperature than 85°C could advance the crosslinking reaction of the matrix which explains the choice behind the 70°C isothermal hold expanded to 50 min. The compaction process is assumed to be correlated to the impregnation of the fiber bed and voids suppression since visual observation of cured specimens did not reveal any resin leakage. The microstructure of an uncured prepreg sample had already been studied by optical microscopic Zeiss Axio Observer in order to investigate the initial state of a stacking sequence of 30 plies $[0]_{30}$ sample debulked under vacuum bag for 2 hours. Fig. 8 displays an optical micrograph taken along its thickness. The microscopic inspection of this section reveals 2 types of voids: voids between plies which were mechanically entrapped during the lay-up and an important amount of dry fibers regions including micro-voids within the core of plies. A comparison with an optical micrograph of a cured sample according to cycle II is presented in Fig. 9. We clearly notice the absence of the dry fibers regions with barely some micro-voids within the core of the ply. Almost no voids are present in the resin interlayer between plies. We presume that only capillary pressure could be the driving force to enhance resin infiltration as the viscosity drops while heating and the compaction mechanism could only be ascribed to the consolidation of the material as been outlined in the introduction and been

reported in recent research works carried out on toughened prepregs [6, 32, 33]. The estimated strains are therefore zeroed at the end of stage 1 considered as a preconditioning region of the material state.

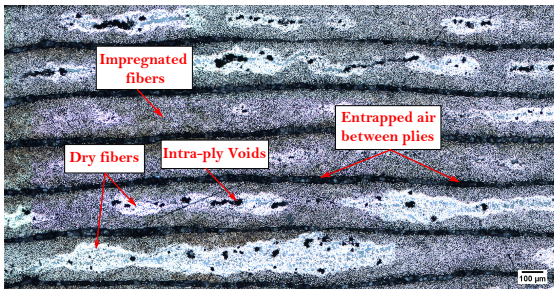

Figure 8: Optical micrograph of an uncured sample microstructure through its thickness.

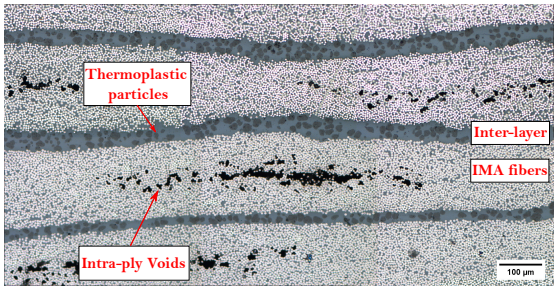

Figure 9: Optical micrograph of a cured sample microstructure through its thickness.

During **'stage 2'** the material is heated from 70°C to 160°C. As can be seen from Fig. 7, the evolution of the estimated degree of cure proves that the material remain uncured up to 145°C. The increase in transverse strains is only driven by thermal effects. We assume that compaction at this stage has already stopped. The material expands more through the thickness than in the in-plane transverse direction thus showing an anisotropic thermal expansion behavior. Along the axial direction, the material does not expand further and the ε_{11} strains remain constant. This stage will be of use to estimate the CTE of the uncured material in next section. During **'stage 3 '** an isothermal dwell is applied at 160°C during 210 min. The whole polymerization reaction takes place during this stage. Transverse strains evolution is directly linked to the

chemical shrinkage of the material. A large drop is visible in the through-thickness direction while it is less drastic in the in-plane direction approving the anisotropic behavior of the material. The change in deformation through the longitudinal direction is rather insignificant during the isothermal dwell. In section 4.4, this stage will be further analyzed in order to quantify the chemical shrinkage response of the prepreg, its dependency on temperature and degree of cure and thus to estimate the CCS. **'Stage 4 '** depicts the material behavior during the cool-down step. The transverse strains drop is due only to thermal contractions. Strains along the axial direction show however a slight increase during cooling related to the negative CTE of the IMA carbon fibers. The estimation of the CTE in the solid state are gathered in next section.

4.3. Thermal expansion behavior and CTE measurements

In Fig. 10 we present the induced strains along both transverse directions and their evolution with the thermal cycle. The curing behavior of sample 2 is taken as an example. As the material is heated, we can notice the through-thickness compaction that starts when the temperature reaches approximately 50°C. Along the transverse in-plane direction, the material expands and somewhat follows the thermal cycle up to 70°C. Indeed, throughout the compaction stage, the transverse in-plane behavior still needs more investigations to further understand the origin of the induced strains whether they are only due to the thermal effects or there is also an induced expansion related to the through-thickness compaction. Nevertheless, this effect seems to be negligible compared to the compaction phenomenon. The CTE at the uncured state (denoted CTE^{Liquid}) of the material can be estimated among its expansion during stage 2. As we can see from Fig. 10 during the heating ramp, the increase in both ε_{22} and ε_{33} is only linked to the temperature increment. The slopes of the linear zones represent the CTE of the material in its liquid state. During the isothermal dwell at 160°C we can notice the strain drop which is driven by the crosslinking reaction of the matrix. During the cooling step, the only prominent phenomenon is the thermal contraction of the prepreg illustrated by

the decrease in both strains ε_{22} and ε_{33}. The value of the glass transition at the end of cure predicted by the kinetics model (Eq. (1)) for samples cured according to cycle II is T = 158°C. The slopes of the linear regressions during cooling from 160°C to ambient temperature give therefore the CTE of the cured glassy state of the prepreg (denoted as CTE^{Glassy}). The values of the CTE at both states were calculated through the curing of all the tested samples (1 - 4) and the average values are gathered in (Table 3).

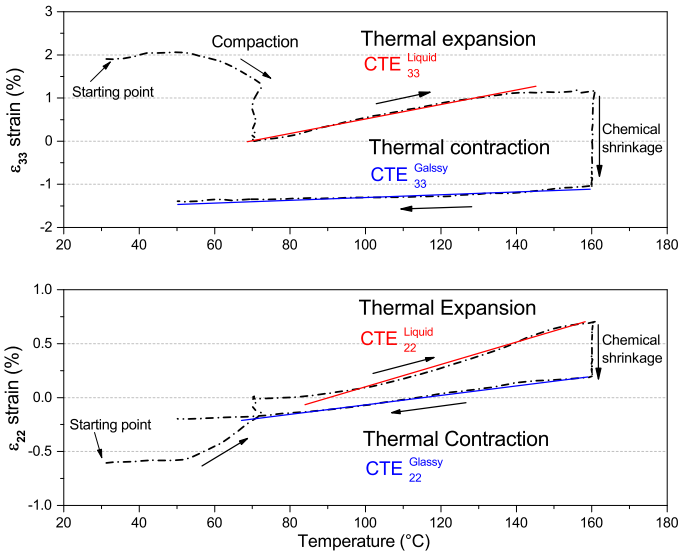

Figure 10: The induced strains along both transverse directions during curing of sample 2 as function of the thermal cycle.

Table 3: Estimated values by the PvT-HADDOC of the CTE for the IMA/M21 material.

$10^{-6}K^{-1}$	CTE Through-thickness	CTE In-plane
Uncured Liquid state	178±9	110±11
Cured Glassy state	55±4	39±4
Comparison with linear dilatometer measurements		
Cured Glassy state	52±1	39±1

The estimated values of the CTE through the thickness are proved to be

higher than the in-plane direction at the liquid state even when the material is fully cured. Such results support previous observations as it was clearly visible in Fig. 7 that during stage 2 the material expanded more along its thickness but also more thermal contraction along direction 3 was observed throughout stage 4. This demonstrates that the IMA/M21 prepreg investigated in this research is rather an orthotropic material than transversely isotropic, contrary to what a UD stacking may suggest. As the reported works in literature lack such *in-situ* multi-axial characterizations and due to the limitations of the used techniques to capture the liquid expansion of toughened prepregs, the material behavior is commonly considered as transversely isotropic. Considering the reported results in this study, one can presume that the orthotropic behavior of the unidirectional IMA/M21 prepreg is arisen from the presence of the extra inter-leaf layers of resin between the fiber rich prepreg plies. In such case, the laminate could not exhibit a symmetric structure in the fiber direction which may explain the variation of the measured properties along both transverse directions. This assumption has been already supported by recent research work that was interested in modeling the behavior of interlayer toughened prepregs. The measurements of the CTE conducted on cured UD laminate samples with linear dilatometer along the transverse directions showed indeed an orthotropic behavior [34].

The CTE of the cured tested samples in this work were also measured using a linear dilatometer Linseis L 75 HXLT. Both transverse directions were investigated using specimens that were cut from each laminate sample after curing. The samples were heated from ambient temperature up to 200°C with a heating rate of 2°C/min. A typical variation of the induced linear expansion of specimens extracted from sample 2 is illustrated in Fig. 11 as a function of temperature. Along the longitudinal direction, the measurements of ε_{11} strain do not reveal any expansion of the material during heating but rather a slight contraction of about zero that could not be noticeable and which is in accordance with the observed tendency of the axial strain measured with the PvT-HADDOC device. Along both transverse directions, the strains evolution

exhibit a change in slope approximately around Tg = 155°C which reflects the differences between the liquid and rubbery expansion coefficients. The point at which the strains change matches perfectly the predicted glass transition temperature. The estimated values of the CTE in the glassy state were compared to the measurements of the PvT-HADDOC device. According to the results gathered in Table. 3, the measurements of the CTE with both methods are in excellent agreement. Similar behavior in the cured state was found in a recent research work [35] conducted on an interlayer toughened UD prepreg using TMA technique showed indeed the orthotropic CTEs of this material. These reported results could validate again the assumption that the presence of the extra layers of resin is the major reason behind the orthotropic behavior of the studied material.

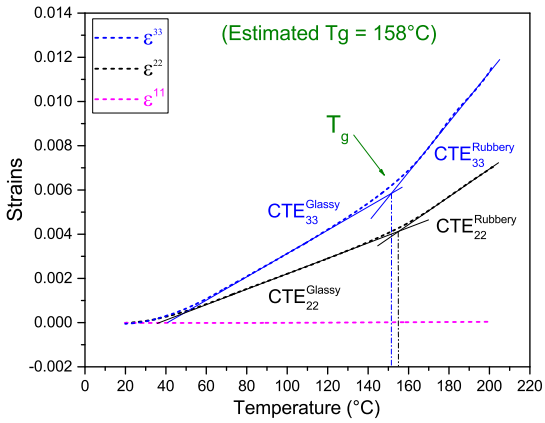

Figure 11: Thermal expansion along both transverse directions of the cured sample 2 measured with linear dilatometer.

4.4. Chemical shrinkage behavior and CCS measurements before / post gelation

The dimension changes of the material that take place during the isothermal hold at stage 3 are directly generated by the crosslinking reaction of the matrix. The chemical shrinkage is a reflection of this reaction and therefore it is much more useful to elaborate the relationship of cure shrinkage with the degree of cure. We assume that during the isothermal dwell there is no effect of thermal

expansion of the material and thereby the measured strains during stage 3 are mainly related to the chemical shrinkage (denoted $\Delta\varepsilon^{chem}$). In Fig. 12, the effect of curing along both transverse directions is isolated and zeroed at the beginning of the isothermal cure at 160°C. The induced strains from the curing of sample 2 are taken as example and presented as a function of the estimated degree of cure. As illustrated in Fig. 12, the dependence of the chemical shrinkage on the degree of cure follows as expected a linear trend but it exhibits a change of slope around a specific point. As reported in [26], the gel point of the M21 system is estimated between $\alpha = 0.51$ and 0.55. Therefore, we assume that the deviation of the chemical shrinkage is attributed to the gelation of the matrix. The slope of each linear region gives the CCS of the unidirectional laminate and hence allows for two coefficients of cure shrinkage to be found along both transverse directions as described below where 'BG' refers to before gelation stage and 'PG' denotes the post gelation one:

$$\Delta\varepsilon^{Chem} = CCS \cdot \Delta\alpha \tag{3}$$

$$CCS_{ii} = \begin{cases} CCS_{ii}^{BG} & \text{if } \alpha < \alpha_{gel} \quad \text{and} \quad ii = 22, 33 \\ CCS_{ii}^{PG} & \text{if } \alpha \geq \alpha_{gel} \quad \text{and} \quad ii = 22, 33 \end{cases}$$

The CCSs presented in Fig. 12 describe the chemical behavior of sample 2. As it is visible, the material does not display the same behavior through both transverse directions. Firstly and in line with the previous results, the chemical strains evolution proves the orthotropic behavior of this unidirectional laminate. The total shrinkage through the thickness direction reaches -2.29% whereas the material only shrank of about -0.5% in the plane direction. Like for CTEs, the presence of interlayers can also explain such behavior even if there is no reported data in the literature that allows a comparison between the chemical shrinkage of toughened prepregs along both transverse directions. All available methods enable measurements along only one direction. Secondly, the estimated values of the CCS reveal an unusual behavior that, to our knowledge, has not been captured before according to the reported works in literature, simultaneously along both directions. Before the gelation, the material tends

to shrink entirely through its thickness with a higher rate of -4% comparing to the in-plane direction where the shrinkage evolves steadily with only -0.33% of rate. With further increase of degree of cure, the rate of the chemical shrinkage increases in the in-plane direction and still shows a linear relation with the degree of cure with a rate of -1.38%. However, through the thickness direction the after gelation behavior is rather characterized by a much slower kinetics with a CCS of -2.06% which is almost half of the CCS before gelation.

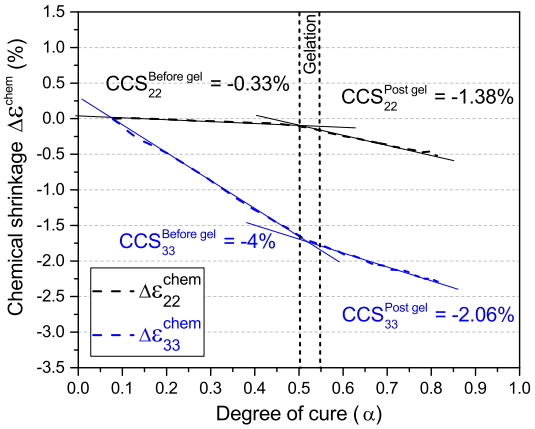

Figure 12: Measured chemical shrinkage of sample 2 during the isotherm cure at 160°C.

The effect of the curing temperature was also studied to further understand the shrinkage behavior. Sample 1 was cured under an isothermal dwell at 180°C. In the same manner, the induced strains captured during the isotherm hold were extracted from the overall induced strains to represent the chemical shrinkage only. In Fig. 13 are illustrated the chemical induced shrinkages along the through thickness direction and along the in-plane direction, respectively, for the two cure temperatures. The estimated values of the CCS along each direction and for each temperature are presented on these graphs. Results show that for a given direction, the chemical shrinkage kinetics follows the same trend regardless of the hold temperature. These expected results support previous reported observations in literature that assume that the cure shrinkage is only a function of the degree of cure regardless of the cure temperature and time

[19, 36]. Consequently, it is possible to estimate average values of the calculated CCS for all the tested samples according to both cure temperatures which are gathered in Table 4.

Table 4: Estimated values by the PvT-HADDOC device of the CCS for the IMA/M21 laminate.

%	CCS Through-thickness	CCS In-plane
Before gelation	-3.83±0.3	-0.27±0.04
After gelation	-2.07±0.1	-1.4 ±0.09

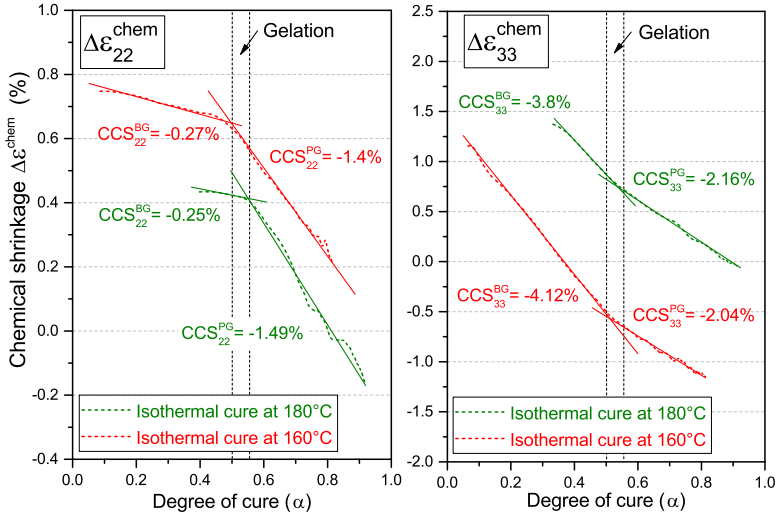

Figure 13: Transverse chemical shrinkage measured during a 180°C and 160°C isothermal cure (Sample 1 and 3 are taken as examples, respectively).

From the results described above, we conclude that thanks to the experimental device used in this work, it was possible to capture in an original and precise way how the material could shrink before and after gelation. In fact, due to the deficiency of the experimental tools commonly used to study the chemical shrinkage of thermoset composites, it has been generally considered that the material shrinks likewise during both regions before and after gel. Shrinkage rate change around the gel point has been already reported in few research works

conducted on pure thermoset epoxy resins [36, 37] or recently on thermosetting composites based on epoxy system [6, 7]. However, their results are not totally in agreement with the findings presented in this work. In a study carried out by Moretti et al. [7] on a similar interlayer toughened prepreg IMA/M21EV using the TMA technique and conducted on samples laid-up in a quasi-isotropic configuration, it was reported that the through-thickness chemical shrinkage follows a completely different behavior. In the pre-gelation region, the material displayed a slow shrinkage rate, whereas after gelation the cure shrinkage progressed with a higher rate. In an other recent research work by Duffner [6], the investigation was conducted on unidirectional samples made of the AS4/8552 prepreg system with dissolved thermoplastic particles that are rather dispersed within plies throughout the bulk phase of the epoxy resin. Thus, the laminate could be considered as transversely isotropic since it does not include resin interlayers between the prepreg plies. Only the in-plane chemical shrinkage was measured through curing and the obtained results showed a similar behavior compared to the studied material in this work. The average value of the pre-gelation CCS was found to be equal to -0.68% and the post gelation CCS to -1.45% which is comparable to the values of the CCS measured along the in-plane direction in this work. Considering the results reported by the above-mentioned authors in addition to the present work, one could assume that the change in the chemical shrinkage rate at the gel point could be only related to the laminate stacking sequence and the fiber bed behavior. In fact, the cure shrinkage behavior of the investigated neat resin did not exhibit any shrinkage rate change around the gel point as reported by Abou Msallem et al. [26]. Besides, as the studied AS4/8552 prepreg does not include extra-interlayers, the change of the cure shrinkage rate cannot be explained by the presence of these interleaves. At the pre-gelation stage, the viscosity of the resin is much lower compared to the post gelation region during which the matrix modulus is assumed to be built. We can suppose that the chemical shrinkage could be correlated to the viscosity of the resin and hence at the pregelation stage, the resin ability to move the fiber bed is likely to be more difficult in the in-plane direction. After gelation, the resin could easily

pull the fibers in the in-plane direction which therefore may explain the increase of the chemical shrinkage rate in this region (CCS post gel).

5. Conclusions

The whole cure behavior of an interlayer toughened Carbon fiber/Epoxy unidirectional composite was investigated in this work. Thanks to the novel experimental bench enabling a homogeneous controlled thermal and mechanical state, it was possible to cover all the cure stages of the studied material. In fact, the laminate consolidation throughout the uncured state was captured, the thermal expansion/ contraction during the heating stages and also the whole chemical shrinkage, *i.e.*, before and post gelation were measured. The analysis of the multi-axial measurements of the thermo-chemical strains allowed us to depict the complex behavior of this third generation unidirectional prepreg that was proved to be rather fully orthotropic due to the presence of the extra resin interlayers between the fiber rich prepregs plies. The consolidation of the uncured material was captured through the compaction mechanism that took place along the through-thickness direction only during the first stage of heating. Such phenomenon was assumed to be correlated to the impregnation of fibers and voids suppression. The manufacturer thermal cycle was adjusted in order to enable the assessment of the thermal expansion of the liquid material. Thus, the suggested two curing cycles allowed us to separate the coupled phenomena, *i.e.*, consolidation and thermal expansion and therefore to measure the CTEs of the uncured material along both transverse directions. The CTEs in the cured state were also estimated by analyzing the material behavior during the cooling step. As a perspective for future research, further investigations will be carried out in order to determine the evolution of the CTE through the full cure along both transverse direction, *i.e.* in the rubbery state. The measured chemical shrinkage of the studied IMA/M21 prepreg revealed the importance of such original *in-situ* multi-axial characterization. It was proved that the UD laminate does not shrink likewise before and after gelation along both transverse

directions contrary to what has been commonly assumed. Indeed, the linear dependency of the chemical shrinkage on the degree of cure exhibits a change of slope around the gel point. Before gelation, the material was entirely contracted through its thickness with an average chemical shrinkage of -1.5 % compared to only -0.1 % along the in-plane transverse direction. However, after the matrix gelation, the through-thickness behavior was rather characterized by a slower shrinkage kinetics. Conversely, the in-plane cure shrinkage rate described by the CCS increased with further increase of the degree of cure. Such complex shrinkage behavior showed an independence on the curing temperature. It was mainly attributed to the role of the fibers in-plane distribution that can lead to such an asymmetric tensile versus compressive behavior as long as the resin is in the uncured state.

Those results clearly show that, for this type of materials, existing thermo-chemo-mechanical models should be improved in order to develop reliable simulation tools for the prediction of residual stresses and process-induced shape distortions.

6. Acknowledgements

The authors would like to acknowledge Hexcel Industries for supplying the material. The authors would also like to thank Nicolas Lefevre for the help on the designing and machining of the experimental bench. We thank Dr Violaine Le Louët, from Capacités SAS, the Engineering and Research valuation subsidiary of the University of Nantes, for her help with the characterization of the neat resin behavior during cure using the PvT-α mold.

[1] Hexcel. Hexcel ready to fly on the A350 XWB. *Reinforced Plastics*, 57(3): 25–26, may 2013. ISSN 00343617. doi: 10.1016/S0034-3617(13)70089-4.

[2] D. Tilbrook, D. Blair, M. Boyle, and P. MacKenzie. Composite materials with blend of thermoplastic particles, 2010.

[3] Toshio Tanimoto. Improving the fatigue resistance of carbon/epoxy laminates with dispersed-particle interlayers. *Acta Materialia*, 46(7):2455–2460, 1998. ISSN 13596454. doi: 10.1016/S1359-6454(98)80028-1.

[4] Ismet Baran, Kenan Cinar, Nuri Ersoy, Remko Akkerman, and Jesper H. Hattel. A Review on the Mechanical Modeling of Composite Manufacturing Processes. *Archives of Computational Methods in Engineering*, 24(2):365–395, 2017. ISSN 18861784. doi: 10.1007/s11831-016-9167-2.

[5] Yasir Nawab, Salma Shahid, Nicolas Boyard, and Frédéric Jacquemin. Chemical shrinkage characterization techniques for thermoset resins and associated composites. *Journal of Materials Science*, 48(16):5387–5409, 2013. ISSN 00222461. doi: 10.1007/s10853-013-7333-6.

[6] Caitlin Duffner. *Experimental Study of the Pre-gelation Behaviour of Composite Prepreg*. PhD thesis, University of British Columbia, 2019.

[7] Laure Moretti, Bruno Castanié, Gérard Bernhart, and Philippe Olivier. Characterization and modelling of cure-dependent properties and strains during composites manufacturing. *Journal of Composite Materials*, 2020. ISSN 1530793X. doi: 10.1177/0021998320912470.

[8] Mael Peron. *Mesure et modélisation des phénomènes de retraits anisotropes dans les matériaux composites durant leur mise en forme*. PhD thesis, University of Nantes, 2016.

[9] J.D Russell. Cure shrinkage of thermoset composites. *SAMPE Quarterly (Society of Aerospace Material and Process Engineers)*, 24:2, 1993. ISSN 0036-0821.

[10] Mohamed S. Genidy, Madhu S. Madhukar, and John D. Russell. A new method to reduce cure-induced stresses in thermoset polymer composites, part ii: Closed loop feedback control system. *SAMPE Quarterly (Society of Aerospace Material and Process Engineers)*, 34:1905–1925, 2000. ISSN 0021-9983. doi: 10.1106/3M0Y-44XM-6WP8-WT7J.

[11] N Boyard, A Millischer, V Sobotka, JL Bailleul, and D Delauny. Behaviour of a moulded composite part: Modelling of dilatometric curve (constant pressure) or pressure (constant volume) with temperature and conversion degree gradients. *Composites Science and Technology*, 67(6):943–954, may 2007. ISSN 02663538. doi: 10.1016/j.compscitech.2006.07.004.

[12] Yasir Nawab, Xavier Tardif, Nicolas Boyard, Vincent Sobotka, Pascal Casari, and Frédéric Jacquemin. Determination and modelling of the cure shrinkage of epoxy vinylester resin and associated composites by considering thermal gradients. *Composites Science and Technology*, 73(1):81–87, 2012. ISSN 02663538. doi: 10.1016/j.compscitech.2012.09.018.

[13] Yasir Nawab, Nicolas Boyard, and Frédéric Jaquemin. Effect of pressure and reinforcement type on the volume chemical shrinkage in thermoset resin and composite. *Journal of Composite Materials*, 48(26):3191–3199, 2014. ISSN 1530793X. doi: 10.1177/0021998313502692.

[14] Nuri Ersoy and Mehmet Tugutlu. Cure kinetics modeling and cure shrinkage behavior of a thermosetting composite. *Polymer Engineering & Science*, 50(1):84–92, jan 2010. ISSN 00323888. doi: 10.1002/pen.21514.

[15] Haixiao Hu, Shuxin Li, Jihui Wang, Lei Zu, Dongfeng Cao, and Yucheng Zhong. Monitoring the gelation and effective chemical shrinkage of composite curing process with a novel FBG approach. *Composite Structures*, 176: 187–194, sep 2017. ISSN 02638223. doi: 10.1016/j.compstruct.2017.04.051.

[16] Shu Minakuchi, Shoma Niwa, Kazunori Takagaki, and Nobuo Takeda. Composite cure simulation scheme fully integrating internal strain measurement. *Composites Part A: Applied Science and Manufacturing*, 84: 53–63, 2016. ISSN 1359835X. doi: 10.1016/j.compositesa.2016.01.001.

[17] Jung Ting Tsai, Joshua S. Dustin, and Jan Anders Mansson. Cure strain monitoring in composite laminates with distributed optical sensor. *Composites Part A: Applied Science and Manufacturing*, 125(June):105503, 2019. ISSN 1359835X. doi: 10.1016/j.compositesa.2019.105503.

[18] Philippe A. Olivier. A note upon the development of residual curing strains in carbon/epoxy laminates. Study by thermomechanical analysis. *Composites Part A: Applied Science and Manufacturing*, 37(4):602–616, 2006. ISSN 1359835X. doi: 10.1016/j.compositesa.2005.05.006.

[19] Tomasz Garstka, N. Ersoy, K.D. Potter, and M.R. Wisnom. In situ measurements of through-the-thickness strains during processing of AS4/8552 composite. *Composites Part A: Applied Science and Manufacturing*, 38(12): 2517–2526, 2007. ISSN 1359835X. doi: 10.1016/j.compositesa.2007.07.018.

[20] Caitlin Duffner, Navid Zobeiry, and Anoush Poursartip. Examination of pre-gelation behaviour in AS4/8552 prepreg composites. *33rd Technical Conference of the American Society for Composites 2018*, 2:880–892, 2018. doi: 10.12783/asc33/25974.

[21] T. G. Gutowski, Z. Cai, S. Bauer, D. Boucher, J. Kingery, and S. Wineman. Consolidation Experiments for Laminate Composites. *Journal of Composite Materials*, 21(7):650–669, 1987. ISSN 1530793x. doi: 10.1177/002199838702100705.

[22] Pascal Hubert and Anoush Poursartip. A Review of Flow and Compaction Modelling Relevant to Thermoset Matrix Laminate Processing. *Journal of Reinforced Plastics and Composites*, 17(4):286–318, mar 1998. ISSN 0731-6844. doi: 10.1177/073168449801700402.

[23] Pascal Hubert and Anoush Poursartip. Aspects of the compaction of composite angle laminates: an experimental investigation. *Journal of Composite Materials*, 35(1):2–26, 2001. ISSN 00219983. doi: 10.1106/X8D7-PR9V-U6F2-0JEK.

[24] Hexcel Corporation. HexPly ® M21 datasheet, 2015.

[25] Y. Ledru, G. Bernhart, R. Piquet, F. Schmidt, and L. Michel. Coupled visco-mechanical and diffusion void growth modelling during composite

curing. *Composites Science and Technology*, 70(15):2139–2145, 2010. ISSN 02663538. doi: 10.1016/j.compscitech.2010.08.013.

[26] Y. Abou Msallem, F. Jacquemin, N. Boyard, A. Poitou, D. Delaunay, and S. Chatel. Material characterization and residual stresses simulation during the manufacturing process of epoxy matrix composites. *Composites Part A: Applied Science and Manufacturing*, 41(1):108–115, 2010. ISSN 1359835X. doi: 10.1016/j.compositesa.2009.09.025.

[27] J Bailleul, G Guyonvarch, B Garnier, Y Jarny, and D Delaunay. Identification des propriétés thermiques de composites fibres de verre/résines thermodurcissables Application à l'optimisation des procédés de moulage. *Revue Générale de Thermique*, 35(409):65–76, 1996. ISSN 00353159. doi: 10.1016/S0035-3159(96)80047-X.

[28] J. P. Pascault and R. J. J. Williams. Glass transition temperature versus conversion relationships for thermosetting polymers. *Journal of Polymer Science Part B: Polymer Physics*, 28(1):85–95, jan 1990. ISSN 08876266. doi: 10.1002/polb.1990.090280107.

[29] Mael Péron, Vincent Sobotka, Nicolas Boyard, and Steven Le Corre. Bulk modulus evolution of thermoset resins during crosslinking: Is a direct and accurate measurement possible? *Journal of Composite Materials*, 51:463–477, 2017. ISSN 1530793X. doi: 10.1177/0021998316647119.

[30] Mael. Péron, Romain. Cardinaud, Nicolas. Lefèvre, Julien. Aubril, Vincent. Sobotka, Nicolas. Boyard, and Steven. Le Corre. PvT-HADDOC: A multi-axial strain analyzer and cure monitoring device for thermoset composites characterization during manufacturing. *Composites Part A: Applied Science and Manufacturing*, 101:129–142, oct 2017. ISSN 1359835X. doi: 10.1016/j.compositesa.2017.06.004.

[31] Basile De Parscau du Plessix, Patrice Lefébure, Nicolas Boyard, Steven Le Corre, Nicolas Lefèvre, Frédéric Jacquemin, Vincent Sobotka, and Sabine

Rolland du Roscoat. In situ real-time 3D observation of porosity growth during composite part curing by ultra-fast synchrotron X-ray microtomography. *Journal of Composite Materials*, 53(28-30):4105–4116, 2019. ISSN 1530793X. doi: 10.1177/0021998319846260.

[32] Navid Zobeiry and Caitlin Duffner. Measuring the negative pressure during processing of advanced composites. *Composite Structures*, 203(June):11–17, 2018. ISSN 02638223. doi: 10.1016/j.compstruct.2018.06.123.

[33] Léonard SERRANO. *Systèmes époxyde - Cuisson hors autoclave et basse température*. PhD thesis, University of Toulouse, 2018.

[34] Tim Frerich, Christian Brauner, Jörg Jendrny, and Axel S. Hermann. Modeling the influence of interleaf layers in composite materials on elastic properties, thermal expansion, and chemical shrinkage. *Journal of Composite Materials*, 53(17):2415–2428, jul 2019. ISSN 0021-9983. doi: 10.1177/0021998319830165.

[35] Laure Moretti. *Simulation des distorsions de cuisson de pièces composites élaborées par co-bonding en autoclave*. PhD thesis, University of Toulouse, 2019.

[36] Chun Li, Kevin Potter, Michael R. Wisnom, and Graeme Stringer. In-situ measurement of chemical shrinkage of MY750 epoxy resin by a novel gravimetric method. *Composites Science and Technology*, 64(1):55–64, 2004. ISSN 02663538. doi: 10.1016/S0266-3538(03)00199-4.

[37] H. Yu, S. G. Mhaisalkar, and E. H. Wong. Cure shrinkage measurement of nonconductive adhesives by means of a thermomechanical analyzer. *Journal of Electronic Materials*, 34(8):1177–1182, 2005. ISSN 03615235. doi: 10.1007/s11664-005-0248-5.